VI. FUGW

Fused Unbalanced Gromov Wasserstein (FUGW) is an approach for aligning pairwise brains based on optimal transformation. We rewrite the Equation (1) of FUGW in [1] as

$$\begin{aligned}\text{FUGW}(\alpha,\beta) :=& \theta \cdot L_W(\mathbf{P}) + (1-\theta)\cdot L_{GW}(\mathbf{P}) + \rho_1 \cdot KL(\mathbf{P}\mathbf{1}|\boldsymbol{\omega}^s) \\ &+ \rho_2 \cdot KL(\mathbf{P}^T\mathbf{1}|\boldsymbol{\omega}^t) + \epsilon \cdot E(\mathbf{P}),\end{aligned} \tag{10}$$

where the term $L_W(\mathbf{P})$ maintains the functional information, the $L_{GW}(\mathbf{P})$ preserves the anatomical structure, and θ makes a trade-off between anatomical structure and functional information; moreover, ρ_1, ρ_2 is used to penalize the margin violations, and $E(\mathbf{P})$ is the entropy regularization term. In our experiments, we set $\rho = \rho_1 = \rho_2$.

Its pairwise alignment between α and β is the coupling $\mathbf{P}$ induced by FUGW(α,β). And its corresponding barycenter on $\{\alpha^k\}_{k\in[m]}$ is a measure β that minimizes the following objective

$$\sum_{k=1}^{m} \text{FUGW}(\alpha^k, \beta). \tag{11}$$

VII. Full experiments

This section demonstrates the effectiveness of our method for computing pairwise alignments and barycenter. All experiments are performed on a server equipped with 2.40GHz Intel CPU, NVIDIA GeForce RTX 3090 GPU, 64GB main memory, and Python 3.12. Our RWD is executed on the CPU, while FUGW runs on the GPU. Our implementation utilizes some Python libraries [22]–[24].

Dataset: The Individual Brain Charting (IBC)[5] [25], [26] is a high spatial-resolution, multi-task fMRI dataset. We select 13 subjects from IBC, and 433 fMRI maps for each subject; We call the above data an original dataset $\mathcal{Q}$. To generate a noisy dataset $\mathcal{Q}'$, we add $\zeta = \zeta_\alpha = \zeta_\beta$ mass of artifacts and apply a random rotation to each original image. The proper margin violation is at most 2ζ.

A. Pairwise alignments

Evaluation metrics: (i) $\mathsf{diff}_a := \|\mathbf{P}\mathbf{1} - \mathbf{a}\|_1$ records the deviation of coupling $\mathbf{P}$ from margin $\mathbf{a}$. (ii) $\mathsf{diff}_b := \|\mathbf{P}^T\mathbf{1} - \mathbf{b}\|_1$ records the deviation of coupling $\mathbf{P}$ from margin $\mathbf{b}$. (iii) loss_{align} refers to the average distance between pairwise noisy data.

To demonstrate the performance of our pairwise alignment method, we applied our algorithms to the noisy dataset $\mathcal{Q}'$. Each case involves 13 subjects. Thus, we compute $\frac{13\times 12}{2} = 78$ pairwise alignments between the subjects. The recorded values are the average results for these 78 pairwise alignments. The hyperparameter ρ of FUGW[6] controls the robustness to noise.

Table I shows that our RWD has better alignment quality than FUGW on noisy datasets, and it is robust to rigid transformations. Moreover, our method does not cause excessive margin violation (i.e., $\mathsf{diff}_a = \mathsf{diff}_b \le 2\zeta$).

TABLE III: Comparisons of different alignment methods on noisy dataset. WD is a special case of RWD, where rigid transformation is replaced with identity transformation.

ζ	method	ρ	time(s)	diff_a	diff_b	$\mathsf{loss}_{align}(\downarrow)$
0.1	FUGW	0.02	1626	0.40	0.41	$156.70_{\pm 61.85}$
	FUGW	0.03	1626	0.57	0.55	$150.55_{\pm 59.62}$
	FUGW	0.06	1626	0.59	0.58	$147.28_{\pm 59.99}$
	FUGW	0.13	1616	0.50	0.47	$150.64_{\pm 59.71}$
	FUGW	0.25	1623	0.37	0.37	$151.63_{\pm 61.80}$
	FUGW	0.50	1627	0.28	0.27	$153.14_{\pm 63.16}$
	FUGW	1	1626	0.21	0.21	$154.91_{\pm 63.65}$
	FUGW	2	1626	0.16	0.16	$157.64_{\pm 62.84}$
	WD	None	328	0.20	0.20	$3.35_{\pm 1.12}$
	RWD	None	1475	0.20	0.20	$2.42_{\pm 0.50}$
0.2	FUGW	0.02	2029	0.52	0.47	$172.96_{\pm 67.21}$
	FUGW	0.03	2023	0.60	0.60	$167.30_{\pm 67.81}$
	FUGW	0.06	2021	0.56	0.56	$162.62_{\pm 68.59}$
	FUGW	0.13	2020	0.44	0.45	$157.83_{\pm 64.94}$
	FUGW	0.25	2021	0.33	0.34	$154.73_{\pm 67.28}$
	FUGW	0.50	2023	0.26	0.27	$157.49_{\pm 66.87}$
	FUGW	1	2021	0.20	0.21	$160.16_{\pm 66.20}$
	FUGW	2	2020	0.14	0.16	$159.28_{\pm 66.72}$
	WD	None	398	0.40	0.40	$2.72_{\pm 1.05}$
	RWD	None	1746	0.40	0.40	$2.01_{\pm 0.54}$
0.3	FUGW	0.02	2650	0.52	0.52	$208.50_{\pm 92.33}$
	FUGW	0.03	2651	0.62	0.64	$204.80_{\pm 94.36}$
	FUGW	0.06	2651	0.58	0.59	$196.32_{\pm 93.91}$
	FUGW	0.13	2652	0.46	0.48	$186.11_{\pm 92.22}$
	FUGW	0.25	2652	0.33	0.35	$177.40_{\pm 91.42}$
	FUGW	0.50	2653	0.24	0.27	$173.17_{\pm 91.25}$
	FUGW	1	2651	0.18	0.21	$172.34_{\pm 91.35}$
	FUGW	2	2644	0.13	0.17	$173.02_{\pm 91.79}$
	WD	None	487	0.59	0.59	$3.84_{\pm 2.39}$
	RWD	None	2152	0.59	0.59	$1.74_{\pm 0.73}$

B. Barycenter

Evaluation metrics: (i) diff records the average deviation of couplings from the weights of m input data and the barycenter. (ii) $loss$ represents the cost incurred from the barycenter to the clean data.

Table II shows the results of our barycenter algorithm. We select six data from the noisy dataset $\mathcal{Q}'$ as input. We compare our barycenter method (RWD-BC) with its corresponding version without rigid transformation (WD-BC) and the FUGW-based method (FUGW-BC). Table II shows that our RWD-BC yields a higher quality barycenter across varying levels of noise.

Figures 2 to 4 illustrate the z-scores of the barycenters. Compared to FUGW-BC and WD-BC, our RWD-BC captures finer details. The FUGW-BC, which incorporates an entropy regularization term, exhibits a diffusion-like behavior when applied to voxel fMRI images (as seen in Figure 1). In FUGW [1], this diffusion effect is mitigated by mapping voxel images onto a pre-specified template before calculating the

[5]Its original [25] and extended version [26] includes 12 and 15 subjects, respectively.

[6]Code and additional details for FUGW are available on GitHub: icasp2025.

TABLE IV: Comparisons of different barycenter algorithms on noisy dataset.

ζ	method	ρ	time(s)	diff	$loss(\downarrow)$
0.1	FUGW	4	571	1.11	$66.70_{\pm 26.62}$
	FUGW	8	571	0.64	$67.28_{\pm 26.66}$
	FUGW	12	573	0.42	$67.09_{\pm 26.64}$
	FUGW	16	572	0.31	$67.52_{\pm 26.79}$
	FUGW	20	569	0.24	$67.22_{\pm 26.85}$
	FUGW	24	569	0.20	$67.07_{\pm 27.07}$
	FUGW	28	569	0.17	$67.46_{\pm 26.84}$
	FUGW	32	572	0.15	$67.66_{\pm 26.84}$
	FUGW	36	572	0.14	$67.43_{\pm 27.01}$
	FUGW	40	572	0.12	$67.44_{\pm 26.87}$
	WD	None	125	0.20	$68.37_{\pm 28.54}$
	RWD	None	467	0.20	$8.43_{\pm 0.17}$
0.2	FUGW	4	640	1.18	$24.74_{\pm 5.91}$
	FUGW	8	640	0.73	$24.72_{\pm 5.98}$
	FUGW	12	640	0.48	$23.80_{\pm 6.01}$
	FUGW	16	640	0.35	$23.58_{\pm 5.72}$
	FUGW	20	642	0.27	$23.45_{\pm 5.84}$
	FUGW	24	641	0.22	$23.61_{\pm 5.94}$
	FUGW	28	641	0.19	$23.55_{\pm 5.79}$
	FUGW	32	642	0.16	$23.59_{\pm 6.03}$
	FUGW	36	641	0.15	$23.71_{\pm 5.90}$
	FUGW	40	640	0.13	$23.90_{\pm 5.95}$
	WD	None	139	0.40	$19.20_{\pm 5.52}$
	RWD	None	502	0.40	$1.10_{\pm 0.11}$
0.3	FUGW	4	731	1.12	$160.09_{\pm 43.12}$
	FUGW	8	732	0.82	$132.55_{\pm 39.10}$
	FUGW	12	732	0.56	$117.68_{\pm 36.00}$
	FUGW	16	732	0.40	$111.21_{\pm 34.96}$
	FUGW	20	732	0.31	$108.37_{\pm 34.58}$
	FUGW	24	731	0.25	$107.41_{\pm 34.69}$
	FUGW	28	732	0.21	$106.96_{\pm 34.41}$
	FUGW	32	730	0.18	$106.39_{\pm 34.50}$
	FUGW	36	731	0.16	$105.28_{\pm 34.50}$
	FUGW	40	732	0.14	$105.26_{\pm 34.40}$
	WD	None	148	0.60	$94.73_{\pm 32.63}$
	RWD	None	562	0.60	$1.19_{\pm 0.12}$

barycenter, making the method dependent on pre-specified template. In contrast, our method does not include the entropy regularization term, allowing it to directly handle voxel images without the need for pre-specified templates.

In conclusion, our method achieves better alignment quality and produces a finer barycenter without relying on any pre-specified template. Moreover, it eliminates the need for tuning the parameter ρ to handle varying levels of noise and does not result in excessive marginal violations. Additionally, our algorithm is more computationally efficient on a CPU than FUGW on a GPU, saving both time and hardware resources.

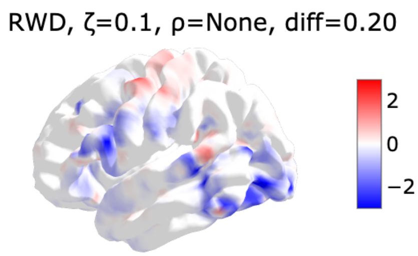

(a) RWD-BC

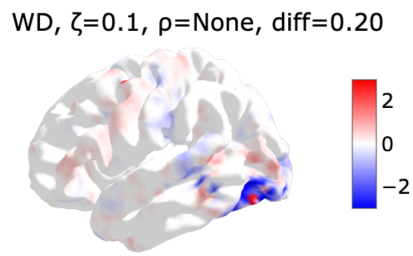

(b) WD-BC

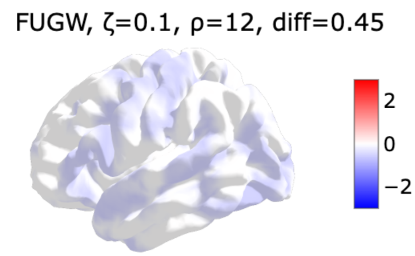

(c) FUGW-BC

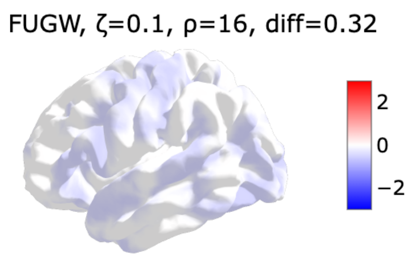

(d) FUGW-BC

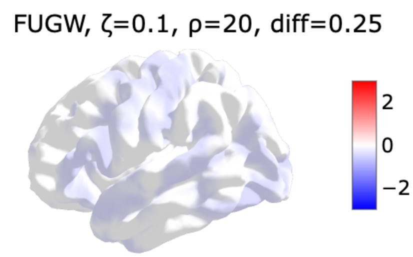

(e) FUGW-BC

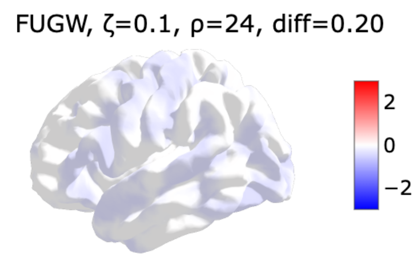

(f) FUGW-BC

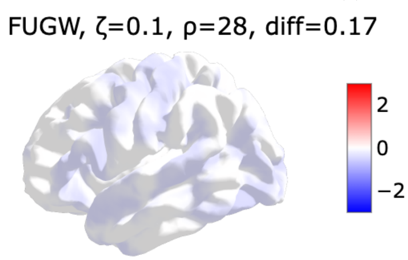

(g) FUGW-BC

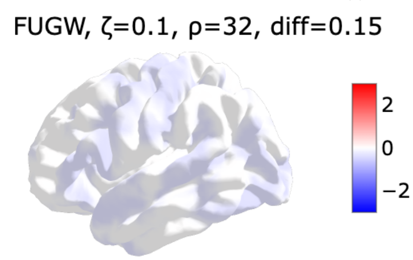

(h) FUGW-BC

Fig. 2: z-score of barycenters with $\zeta = 0.1$.

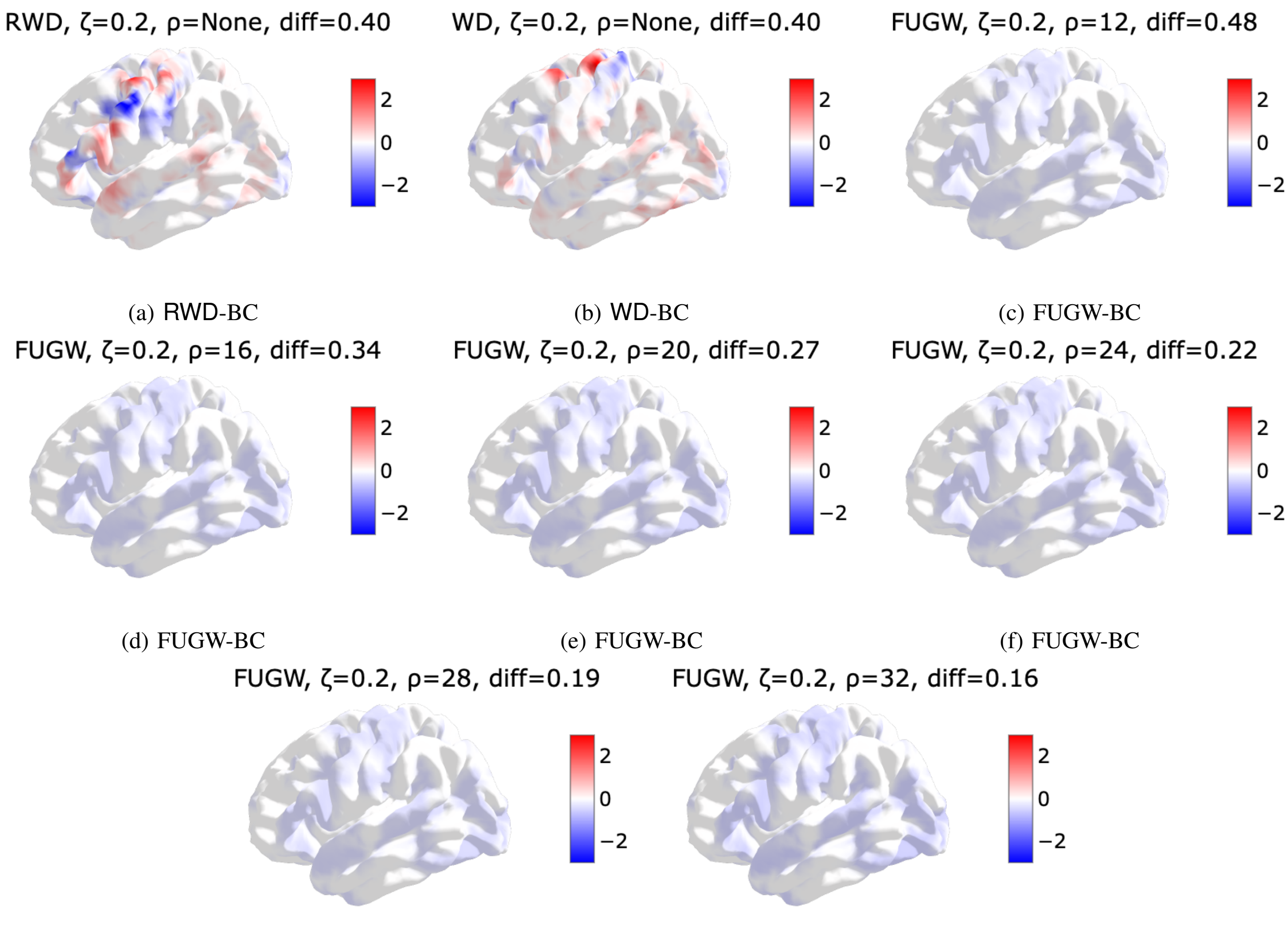

(a) RWD-BC (b) WD-BC (c) FUGW-BC

(d) FUGW-BC (e) FUGW-BC (f) FUGW-BC

(g) FUGW-BC (h) FUGW-BC

Fig. 3: z-score of barycenters $\zeta = 0.2$.

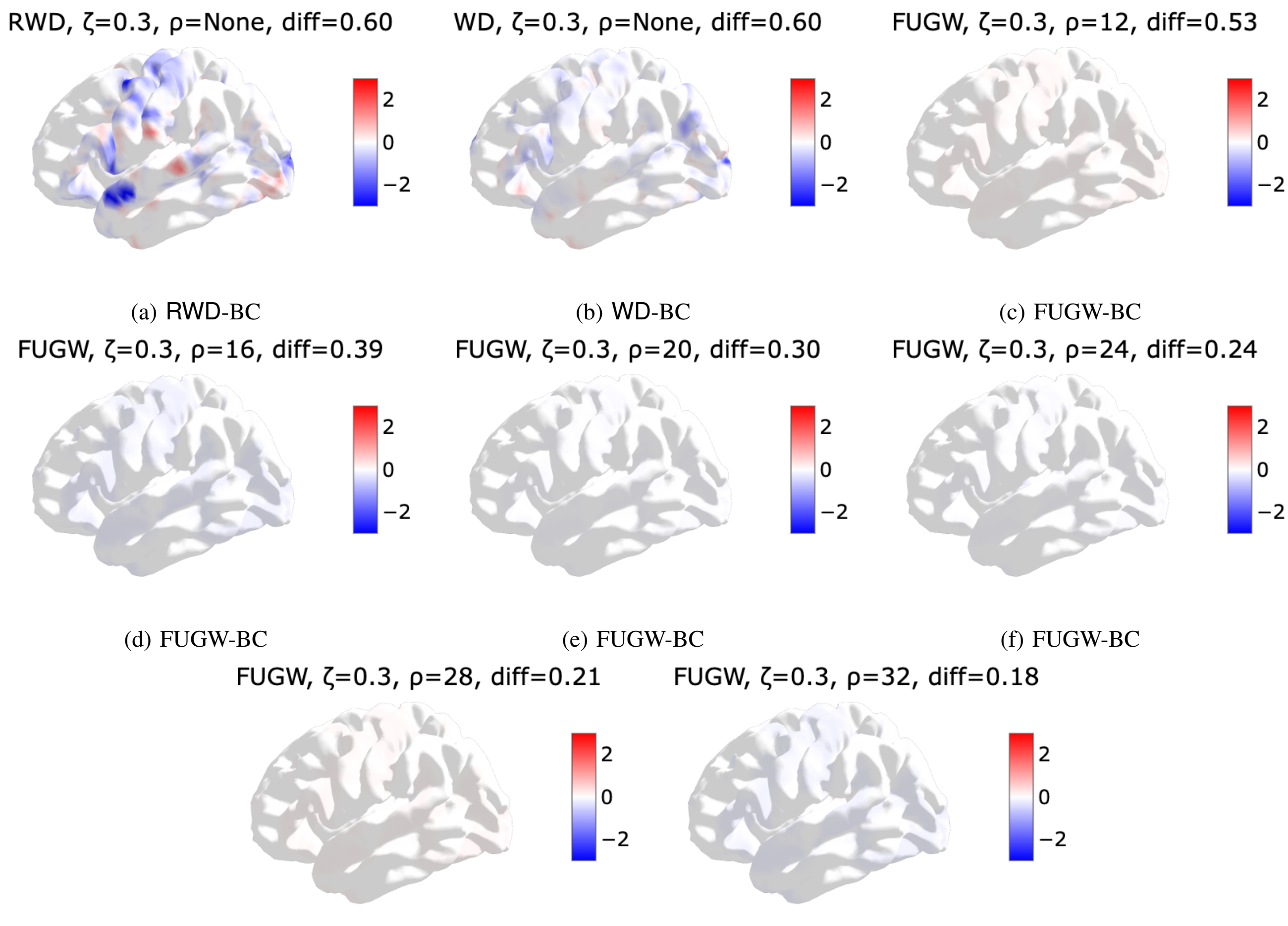

(a) RWD-BC (b) WD-BC (c) FUGW-BC

(d) FUGW-BC (e) FUGW-BC (f) FUGW-BC

(g) FUGW-BC (h) FUGW-BC

Fig. 4: z-score of barycenters $\zeta = 0.3$.